Helical Structures

DOI: 10.1002/anie.200700891

Helical Arrangement of Interstrand Stacked Pyrenes in a DNA Framework**

*Vladimir L. Malinovskii, Florent Samain, and Robert Häner**

DNA plays an eminent role in the construction of well-defined nanostructures and nanodevices.[1] The unique feature of self-organization, combined with the ease of automated oligonucleotide synthesis,[2] has driven the rapid progress in DNA nanotechnology.[3] On the other hand, possible medical and materials applications may be limited by the chemical and physical properties of the natural DNA building blocks. Not surprisingly, the quest for modified building blocks that have the required properties is continuing with high intensity.[4] Ever since the discovery of the DNA double helix, the generation of helical structures that are not based on the hydrogen-bond-mediated pairing scheme of the nucleobases or related derivatives has been a highly competitive aspect in the field of molecular self-organization.[5] Novel types of artificial helical structures may find applications in the area of molecular electronics,[3a,b] they may lead to the generation of nanomechanical devices,[3g,h,i] diagnostic applications,[3j] or to systems with biomimetic functions.[3d,f] The recognition motifs utilized so far to create double-stranded assemblies can be grouped into ligand-to-metal coordination, hydrogen-bonding, aromatic stacking, and electrostatic interactions.[6] While a range of reports describe the formation of foldamers with aromatic building blocks in organic media, the number of accounts on such systems in aqueous conditions is limited.[7] The development of methods that lead to functional artificial double-helical structures is, thus, still a major challenge.[8] Herein we present a highly ordered structure which is formed by simple pyrene building blocks. The system represents the first example of an interstrand helical organization within an entirely artificial section embedded in a double-stranded DNA molecule. Moreover, the observed double-helical structure is formed under physiologically compatible conditions.

The constructs are composed of achiral, non-nucleosidic pyrene building blocks (**S**), which are embedded in a DNA (Figure 1). The incorporation of non-nucleosidic building blocks into oligonucleotides, which was pioneered by the research groups of Letsinger and Lewis,[9] has gained much attention lately.[7c,d,10,11] Our own efforts have involved the assembly of DNA-like structures with polyaromatic derivatives, such as phenanthrene, phenanthroline, and pyrene.[11] A model of interstrand-stacked polyaromatic residues was derived from spectroscopic data.[12] We have subsequently expanded the studies to extended stacks of pyrene building blocks. The corresponding oligomeric compounds **1**–**10** are shown in Table 1. The pyrene residues are contained in the middle of a DNA duplex. The number of pyrene units ranges from 2 (duplex **3**·**4**) to 14 (duplex **9**·**10**). Duplex **1**·**2** serves as the reference.

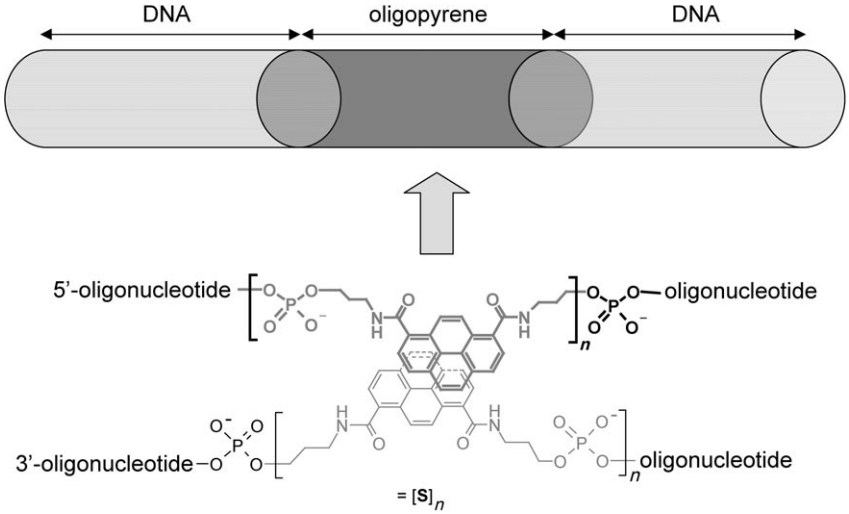

Figure 1. Schematic representation of oligopyrene stacks embedded in a DNA duplex.

The influence of pyrene incorporation on the stability of the hybrids was analyzed by thermal denaturation studies. Table 1 shows the experimental T_m (melting temperature) values as well as the theoretical values for the corresponding hybrids without any contribution from the pyrene residues. The latter value, which was calculated according to the method described by Markham and Zuker,[13] allows an estimation of the contribution of the pyrene groups to the overall stability (ΔT_m). While 2 and 4 pyrene residues add little to the hybrid stability, 6 and 14 pyrene residues have a

[*] Dr. V. L. Malinovskii, F. Samain, Prof. Dr. R. Häner
Departement für Chemie und Biochemie
Universität Bern
Freiestrasse 3, 3012 Bern (Switzerland)
Fax: (+41) 31-631-8057
E-mail: robert.haener@ioc.unibe.ch

[**] Financial support by the Swiss National Foundation (grant 200020-109482) is gratefully acknowledged.

Supporting information for this article (full experimental details) is available on the WWW under http://www.angewandte.org or from the author.

Table 1: Influence of multiple pyrene residues on the thermal stability of hybrids.

	Duplex[a]	T_m [°C] exp.[b]	T_m [°C] calcd[c]	ΔT_m [°C][d]
1	5′ AGCTCGGTCATCGAGAGTGCA	70.5	70.5	–
2	3′ TCGAGCCAGTAGCTCTCACGT			
3	5′ AGCTCGGTCA**S**CGAGAGTGCA	70.1	69.5	+0.6
4	3′ TCGAGCCAGT**S**GCTCTCACGT			
5	5′ AGCTCGGTC**SS**CGAGAGTGCA	68.0	68.1	+0.1
6	3′ TCGAGCCAG**SS**GCTCTCACGT			
7	5′ AGCTCGGT**SSS**CGAGAGTGCA	65.1	47.1	+18.0
8	3′ TCGAGCCA**SSS**GCTCTCACGT			
9	5′ AGCTC**SSSSSSS**GAGAGTGCA	56.5	33.6	+22.9
10	3′ TCGAG**SSSSSSS**CTCTCACGT			

[a] 1.0 μM each strand, 10 mM phosphate buffer, pH 7.0. [b] Experimental error: ±0.5 °C. [c] Calculated T_m values.[13] [d] Difference between the experimental and calculated T_m values.

rather large positive effect on the T_m value of the respective hybrids. This finding indicates that interstrand interactions between the pyrene units lead to a significant stabilization of the duplex. Moreover, intrastrand folding of single strands through pyrene stacking can facilitate duplex formation by reducing the entropy change in a manner similar to single-strand preorganization in natural oligonucleotides.[14] The occurrence of inter- and intrastrand pyrene stacking interactions is supported by temperature-dependent UV/Vis spectroscopic studies, which show the presence of two isosbestic points upon melting of the duplex.[15] Furthermore, signal broadening and hypochromicity, both of which serve as evidence for face-to-face aggregates,[16] were observed upon duplex formation[17] (see the Supporting Information).

Next, the fluorescence properties of the oligomers were analyzed. The single strands containing more than one pyrene moiety (**5**–**10**) and the hybrids formed among them exhibited mainly excimer emission over the temperature range 10–90 °C, and showed—in good agreement with our expectations—that pyrene units are strongly aggregated in single as well as double strands (see the Supporting Information). Some exceptional behavior, however, was observed in the emission spectra of hybrid **9·10**. While hybrids **5·6** and **7·8**[18] show a red shift in the excimer emission upon hybrid formation (see the Supporting Information), hybrid **9·10** behaves in the opposite way. As can be seen in Figure 2, duplex formation leads to a significant blue shift (511 to 504 nm) when going from 90→10 °C. The aggregation of the pyrene units and the resulting changes in the fluorescence properties have been studied in detail and reviewed by Winnik.[19] The inverse behavior of hybrid **9·10** is an indication that a sandwich-type aggregation of pyrene units is restricted within the duplex. The probability of adopting the preferred sandwich-type aggregation increases with rising temperature and flexibility, and furthermore upon strand dissociation. Blue-shifted fluorescence as a result of only partially overlapping excimer geometries has, for example, been observed in crystalline pyrene derivatives, pyrenophanes, bispyrenyl systems, and polymers with twisted or strained pyrene conformations.[19,20] An intriguing interpretation of this behavior is the occurrence of a helical arrangement of the

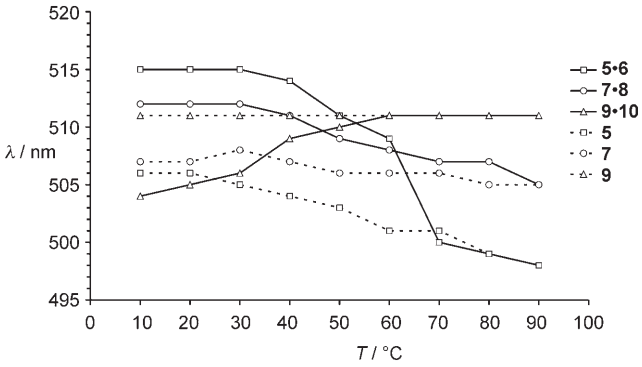

Figure 2. Trends of the excimer fluorescence maxima upon melting of hybrids **5·6**, **7·8**, and **9·10** and single strands **5**, **7**, and **9**.

pyrene moieties in hybrid **9·10**, triggered by the unmodified DNA parts. The twisting of the pyrene units upon adoption of a helical conformation would explain the blue-shifted emission. Indeed, confirmation of a helical arrangement of the interstrand-stacked pyrenes was obtained by circular dichroism (CD) spectroscopy.

The CD spectra of the pyrene-modified hybrid **9·10** and the unmodified DNA duplex **1·2** at room temperature are shown in Figure 3 a. Clearly, the spectrum of **9·10** in the 200–315 nm range is very different from that of B-DNA (**1·2**). The spectrum is dominated by strong dichroism of the pyrene

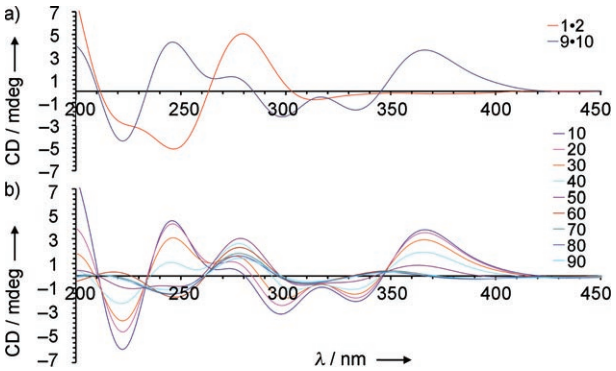

Figure 3. a) CD spectra of natural duplex **1·2** and modified duplex **9·10** at 25 °C; b) temperature-dependent CD spectra of duplex **9·10** (10→90 °C; 1.0 μM solution in phosphate buffer, pH 7.0).

bands, which indicates a well-ordered structure in the oligopyrene region of the duplex. Further evidence for a helical arrangement comes from the very intense bisignate signal for the pyrene band centered at 348 nm, with a positive Cotton effect at $\lambda = 365$ nm ($\Delta\varepsilon = +113\,M^{-1}cm^{-1}$), followed by a minimum at $\lambda = 332$ nm ($\Delta\varepsilon = -62\,M^{-1}cm^{-1}$). Since there is no interference with the nucleobases in this area of the spectrum, the shape of this signal provides valuable insight into the stacking arrangement of the pyrene rings. Thus, a positive amplitude ($A = +175$) obtained from exciton-coupled CD reveals a positive chirality.[21,22] These data suggest that the pyrene units are arranged in a right-handed helical orientation within the oligopyrene stack. The CD couplet in

the pyrene region of the spectrum (350 nm) gradually disappears as the temperature is increased from 10 to 90 °C, and the remaining part of the spectrum adopts the features of a normal B-DNA (see Figure 3b). Bisignate signals of pyrene are not present in the CD spectra of single strands **9** and **10**, which reveals a random aggregation of the pyrene units (see the Supporting Information). Furthermore, the CD spectra of hybrids **3·4**, **5·6**, and **7·9** were also very similar to that of normal B-DNA, with no signs of helicity in the oligopyrene region.

Duplex **9·10** represents a system composed of 28 natural nucleotides and 14 pyrene units. To address the question of the cooperativity of duplex melting, temperature-dependent absorbance was recorded at 354 nm (pyrene absorbance only) and 245 nm (pyrene and nucleobase absorbance). Comparison of these data, together with the already described values obtained at 260 nm, showed excellent agreement (Table 2), thus suggesting a high degree of cooperativity among the different sections of the hybrid.[23]

Table 2: Melting temperatures determined at 245, 260, and 354 nm.

Hybrids	T_m [°C] 245 nm[a]	T_m [°C] 260 nm[a]	T_m [°C] 354 nm[b]
1·2	70.2	70.5	–
3·4	69.9	70.1	70.1
5·6	68.7	68.0	68.0
7·8	65.1	65.1	65.9
9·10	56.3	56.5	55.4

[a] Nucleobase and pyrene absorbance. [b] Pyrene absorbance.

The arrangement of pyrene molecules covalently linked to the sugar backbone in RNA[24] and to base residues in DNA[25] was published recently. In these studies, DNA or RNA were used as structural scaffolds for the helical arrangement of pyrenes. In contrast to these intrastrand helical stacks along a DNA or RNA backbone,[24,25] the present system describes the self-organization of two non-nucleosidic oligopyrene strands in an interstrand helical stack. An Amber-mimized model[26] (Figure 4) shows an overall right-handed helical arrangement of the twisted pyrene rings, which is in agreement with the experimental observations. Since the experiments were carried out in aqueous conditions, the stacking of the pyrene moieties are largely driven by hydrophobic interactions.[27] However, because of the presence of an amide-type linker, hydrogen-bond formation may also play a significant role in the stability as well as for the organization of the helical structure.[28] A crystal structure obtained from the pyrene-1,8-dicarboxylic acid bis[(3-hydroxy-propyl)amide] building block shows the existence of hydrogen bonds between the amide groups of adjacent pyrene units. Furthermore, the pyrene units are stacked in a twisted, face-to-face orientation in the crystal (see the Supporting Information).[29]

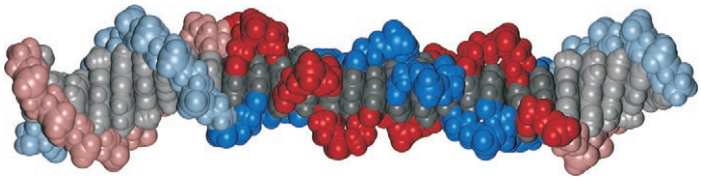

Figure 4. Molecular model of hybrid **9·10**. Oligopyrene regions are shown in dark colors and the flanking DNA regions in light colors (linkers between pyrenes and sugar-phosphate backbones are shown in red and blue, nucleobases and pyrene moieties in gray). The two oligopyrene strands are arranged in a right-handed helix.

In summary, we have reported a self-organizing system composed of two oligopyrene strands that leads to the formation of an interstrand helical stack embedded in a double-stranded DNA. Helical organization, as shown by fluorescence and CD spectroscopy, takes place in a hybrid containing 14 consecutive achiral pyrene building blocks but not within the respective single strands nor in hybrids containing only 6 or less pyrene residues. Interstrand stacking of the pyrene units within the duplex is supported by high duplex stability as well as by UV/Vis and fluorescence spectroscopy. The findings are important for the design of artificial molecular double-stranded helices for applications in nanotechnology.

Received: February 27, 2007

Keywords: DNA · helical structures · nanostructures · pyrenes · stacking interactions

[1] N. C. Seeman, *Nature* **2003**, *421*, 427–431.
[2] M. H. Caruthers, *Science* **1985**, *230*, 281–285.
[3] a) J. R. Heath, M. A. Ratner, *Phys. Today* **2003**, *56*, 43–49; b) M. Taniguchi, T. Kawai, *Phys. E* **2006**, *33*, 1–12; c) K. V. Gothelf, T. H. LaBean, *Org. Biomol. Chem.* **2005**, *3*, 4023–4037; d) J. Wengel, *Org. Biomol. Chem.* **2004**, *2*, 277–280; e) U. Feldkamp, C. M. Niemeyer, *Angew. Chem.* **2006**, *118*, 1888–1910; *Angew. Chem. Int. Ed.* **2006**, *45*, 1856–1876; f) R. Fiammengo, M. Crego-Calama, D. N. Reinhoudt, *Curr. Opin. Chem. Biol.* **2001**, *5*, 660–673; g) K. Kinbara, T. Aida, *Chem. Rev.* **2005**, *105*, 1377–1400; h) E. R. Kay, D. A. Leigh, F. Zerbetto, *Angew. Chem.* **2007**, *119*, 72–196; *Angew. Chem. Int. Ed.* **2007**, *46*, 72–191; i) N. C. Seeman, *Trends Biochem. Sci.* **2005**, *30*, 119–125; j) N. L. Rosi, C. A. Mirkin, *Chem. Rev.* **2005**, *105*, 1547–1562.
[4] a) A. Eschenmoser, *Chimia* **2005**, *59*, 836–850; b) B. Samorí, G. Zuccheri, *Angew. Chem.* **2005**, *117*, 1190–1206; *Angew. Chem. Int. Ed.* **2005**, *44*, 1166–1181; c) P. Herdewijn, *Biochim. Biophys. Acta Gene Struct. Expression* **1999**, *1489*, 167–179; d) O. Köhler, D. V. Jarikote, I. Singh, V. S. Parmar, E. Weinhold, O. Seitz, *Pure Appl. Chem.* **2005**, *77*, 327–338.
[5] a) C. Piguet, G. Bernardinelli, G. Hopfgartner, *Chem. Rev.* **1997**, *97*, 2005–2062; b) S. H. Gellman, *Acc. Chem. Res.* **1998**, *31*, 173–180; c) A. E. Rowan, R. J. M. Nolte, *Angew. Chem.* **1998**, *110*, 65–71; *Angew. Chem. Int. Ed.* **1998**, *37*, 63–68; d) D. J. Hill, M. J. Mio, R. B. Prince, T. S. Hughes, J. S. Moore, *Chem. Rev.* **2001**, *101*, 3893–4011.
[6] a) V. Berl, I. Huc, R. G. Khoury, M. J. Krische, J.-M. Lehn, *Nature* **2000**, *407*, 720–723; b) K. Tanaka, A. Tengeiji, T. Kato, N. Toyama, M. Shionoya, *Science* **2003**, *299*, 1212–1213; c) J.-M. Lehn, A. Rigault, J. Siegel, J. Harrowfield, B. Chevrier, D. Moras, *Proc. Natl. Acad. Sci. USA* **1987**, *84*, 2565–2569; d) Y. Tanaka, H. Katagiri, Y. Furusho, E. Yashima, *Angew. Chem.* **2005**, *117*, 3935–3938; *Angew. Chem. Int. Ed.* **2005**, *44*, 3867–3870; e) E. C. Constable, *Chem. Soc. Rev.* **2007**, *36*, 246–253; f) X. Yang, S. Martinovic, R. D. Smith, B. J. Gong, *J. Am. Chem. Soc.* **2003**, *125*, 9932–9933.

[7] a) G. L. Gabriel, B. L. Iverson, *J. Am. Chem. Soc.* **2002**, *124*, 15174 – 15175; b) J. Lee, V. Guelev, S. Sorey, D. W. Hoffmann, B. L. Iverson, *J. Am. Chem. Soc.* **2004**, *126*, 14036 – 14042; c) W. Wang, W. Wan, H.-H. Zhou, S. Niu, A. D. Q. Li, *J. Am. Chem. Soc.* **2003**, *125*, 5248 – 5249; d) W. Wang, W. Wan, A. Stachiw, A. D. Q. Li, *Biochemistry* **2005**, *44*, 10751 – 10756; e) I. , Huc, V. Maurizot, H. Gornitzka, J.-M. Leger, *Chem. Commun.* **2002**, 578 – 579; f) H. Goto, H. Katagari, Y. Furusho, E. Yashima, *J. Am. Chem. Soc.* **2006**, *128*, 7176 – 7178.

[8] M. Albrecht, *Angew. Chem.* **2005**, *117*, 6606 – 6609; *Angew. Chem. Int. Ed.* **2005**, *44*, 6448 – 6451.

[9] a) R. L. Letsinger, T. Wu, *J. Am. Chem. Soc.* **1995**, *117*, 7323 – 7328; b) F. D. Lewis, R. L. Letsinger, M. R. Wasielewski, *Acc. Chem. Res.* **2001**, *34*, 159 – 170.

[10] a) Y. Zheng, H. Long, G. C. Schatz, F. D. Lewis, *Chem. Commun.* **2005**, 4795 – 4797; b) Y. Zheng, H. Long, G. C. Schatz, F. D. Lewis, *Chem. Commun.* **2006**, 3830 – 3832.

[11] a) S. M. Langenegger, R. Häner, *Helv. Chim. Acta* **2002**, *85*, 3414 – 3421; b) S. M. Langenegger, R. Häner, *Tetrahedron Lett.* **2004**, *45*, 9273 – 9276; c) S. M. Langenegger, R. Häner, *ChemBioChem* **2005**, *6*, 2149 – 2152.

[12] S. M. Langenegger, R. Häner, *Chem. Commun.* **2004**, 2792 – 2793.

[13] N. R. Markham, M. Zuker, *Nucl. Acids Res.*, web server issue **2005**, W577–W581.

[14] E. T. Kool, *Chem. Rev.* **1997**, *97*, 1473 – 1487.

[15] The two single strands **9** and **10** each show a single isosbestic point at 369 nm in temperature-dependent UV/Vis experiments (see the Supporting Information).

[16] a) I. Tinoco, Jr., *J. Am. Chem. Soc.* **1960**, *82*, 4785 – 4790; b) C. R. Cantor, P. R. Schimmel, *Biophysical Chemistry*, *part II*, W. H. Freeman, New York, **1980**, pp. 349 – 408.

[17] Hypochromicity is also observed for the pyrene band at 245 in the pyrene–oligonucleotide overlapping area (210–300 nm, see the Supporting Information).

[18] Duplex **3**·**4** is not included in this comparison because of the transition from monomer to excimer emission upon formation of the hybrid.

[19] F. M. Winnik, *Chem. Rev.* **1993**, *93*, 587 – 614.

[20] for example, a) H. A. Staab, N. Riegler, F. Diederich, C. Krieger, D. Schweitzer, *Chem. Ber.* **1984**, *117*, 246 – 259; b) K. A. Zachariasse, W. Kuhnle, A. Weller, *Chem. Phys. Lett.* **1978**, *59*, 375 – 380; c) T. Kanaya, K. Goshiki, M. Yamamoto, Y. Nishijima, *J. Am. Chem. Soc.* **1982**, *104*, 3580 – 3587; d) M. J. Snare, P. J. Thistlethwaite, K. P. Ghiggino, *J. Am. Chem. Soc.* **1983**, *105*, 3328 – 3332; e) I. Suzuki, M. Ui, A. Yamauchi, *J. Am. Chem. Soc.* **2006**, *128*, 4498 – 4499.

[21] "Positive exciton chirality" is defined as a right-handed twist of the electric transition dipole moments of two chromophores, see N. Berova, K. Nakanishi in *Circular dichroism: principles and applications* (Eds.: N. Berova, K. Nakanishi, R. W. Woody), Wiley-VCH, New York, **2000**, pp. 337 – 382.

[22] For exciton coupling in pyrene-based systems, see for example a) A. Ueno, I. Suzuki, T. Osa, *J. Am. Chem. Soc.* **1989**, *111*, 6391 – 6397; b) O. Shoji, D. Nakajima, M. Ohkawa, Y. Fujiwara, M. Annaka, M. Yoshikunu, T. Nakahira, *Macromolecules* **2003**, *36*, 4557 – 4566.

[23] a) R. Lumry, R. Biltonen, *Biopolymers* **1966**, *4*, 917 – 944; b) J. SantaLucia, Jr. in *Spectrophotometry and spectrofluorimetry, a practical approach* (Ed.: M. G. Gore), Oxford Press, New York **2000**, pp. 329 – 356.

[24] M. Nakamura, Y. Ohtoshi, K. Yamana, *Chem. Commun.* **2005**, 5163 – 5165.

[25] E. Mayer-Enthart, H.-A. Wagenknecht, *Angew. Chem.* **2006**, *118*, 3451 – 3453; *Angew. Chem. Int. Ed.* **2006**, *45*, 3372 – 3375.

[26] *Hyperchem 7.5* (*Hypercube*, Waterloo, Ontario) amber force field minimized structure.

[27] a) E. A. Meyer, R. K. Castellano, F. Diederich, *Angew. Chem.* **2003**, *115*, 1244 – 1287; *Angew. Chem. Int. Ed.* **2003**, *42*, 1210 – 1250; b) J. C. Nelson, J. G. Saven, J. S. Moore, P. G. Wolynes, *Science* **1997**, *277*, 1793 – 1796.

[28] For a recent review, see I. Huc, *Eur. J. Org. Chem.* **2004**, 17 – 29.

[29] CCDC-636616 contains the supplementary crystallographic data for this paper. These data can be obtained free of charge from The Cambridge Crystallographic Data Centre via www.ccdc.cam.ac.uk/data_request/cif.

